European Journal of Remote Sensing - 2016, 49: 417-431
doi: 10.5721/EuJRS20164923
Received 10/02/2016 accepted 14/06/2016

European Journal of Remote Sensing
An official journal of the Italian Society of Remote Sensing
www.aitjournal.com

Railways' stability observed in Campania (Italy) by InSAR data

Davod Poreh*, Antonio Iodice, Daniele Riccio and Giuseppe Ruello

Università degli Studi di Napoli "Federico II",
Dipartimento di Ingegneria Elettrica e delle Tecnologie dell'Informazione,
Via Claudio 21, 80125 Napoli, Italy
*Corresponding author, e-mail address: davod.poreh@unina.it

Abstract
Campania region is characterized by intense urbanization, active volcanoes, subsidence, and landslides; therefore, the stability of public transportation structures is highly concerned. We have applied DInSAR technique to a stack of 25 X-band radar images of Cosmo-SkyMed (CSK) satellites collected over an area in Campania, in order to monitor the railways' stability. The study area was already investigated with older, low-resolution sensors like ERS1/2 and ENVISAT-ASAR before, but the number of obtained persistent scatterers (PSs) was too limited to get useful results. Here, for the first time we apply CSK high resolution imagery to this study area, so obtaining a number of PSs sufficient to detect possible deformations on the railways. We focused on a bridge at Triflisco, over the Volturno River. Our results demonstrate a stable condition. Comparison with the local thermal data shows that the main deformation on the bridge is limited to periodical deformation of the steel structure.
Keywords: Cosmo-SkyMed, subsidence, Synthetic Aperture Radar (SAR), interferometry, Persistent Scatterer Interferometry (PSI).

Introduction
Persistent Scatterer Interferometry (PSI) is a powerful technique that has been employed for more than 15 years for studying/monitoring of soil deformation rates. It uses Interferometric Synthetic Aperture Radar (InSAR) imageries as input. The PSI methodology is particularly suitable to urban regions, rather than to rural areas where the coherency of the radar signals is decreased dramatically. PSI is an advanced, more recent type of Differential Interferometric Synthetic Aperture Radar (D-InSAR) technique. In the traditional D-InSAR data analysis methodologies, temporal decorrelation -decrease of similarity between images-, geometrical decorrelation, and phase delay due to atmospheric effects on Electro-Magnetic (EM) waves, are three major limitations of application. However, for some specific conditions like urban area, highways, or railways, temporal de-correlation decreases dramatically (i.e., coherency is higher), and features remain coherent in the produced interferograms for a long time [Usai and Hanssen, 1997; Ferretti et al., 1999a, 1999b, 2000, 2001]. To overcome

the coherency problems of backscatterers (changes of the backscatters during the time) in repeat pass SAR interferometry, PSI was developed.

Historically speaking, different PSI techniques have been proposed in the last decades. The first PSI technique, named Permanent Scatterers Interferometry, was developed by researchers of the Politecnico di Milano (POLIMI) [Ferretti et al., 2000, 2001]. Soon after, some other similar methodologies have been rapidly developed. The other similar well known time series radar interferometric approach is named Small Baseline Subset (SBAS) [Berardino et al., 2002; Lanari et al., 2004; Pepe et al., 2005, 2007, 2011]. In PSI analysis all acquisitions are employed, whereas in SBAS some of them are not, because their spatial baseline is too high. SBAS methodologies are more sensitive to geometric and temporal decorrelation compared to PSI analysis [Berardino et al., 2002]. In SBAS, much more interferograms are created than in a single master approach (like PSI). The unwrapping procedure for SABAS and PSI is also different. In SBAS, at least in its original implementation, the interferograms are unwrapped first spatially and then temporally, while it is the opposite in the PSI analysis. One of the major disadvantages of SBAS is that in this approach disconnected clusters of interferograms might be obtained in the temporal and perpendicular baseline graphs. However, SBAS allows to measure displacements not only on highly stable point-like scatterers, but also on distributed scatterers (DS), i.e., areas with intermediate coherence. Therefore, several researches have been reported aiming to develop techniques able to combine advantages of both PSI and SBAS. For instance, minimization of the baselines and use of all radar images also in SBAS methodology were proposed in the literature [e.g., Perissin et al., 2008]. Another similar technique for the earth surface's change monitoring was reported in Mora et al. [2003]. A geophysical approach in Hooper et al., 2004 and a stepwise linear deformation with least square adjustment in Crosetto et al. [2005] has been reported. Interferometric Point Target Analysis (IPTA), and stable point networks are reported in Werner et al. [2003] and Crosetto et al. [2008], respectively. In [Hooper et al., 2008] multiple image pixels are used within a certain radius to estimate spatially correlated parameters (e.g., deformation rates, atmospheric signal delay). In this methodology, PSI and small baseline analysis have been combined heuristically. The SqueeSAR algorithm, capable of simultaneous analysis of PSI (i.e., PS) and DS, was reported in [Ferretti et al., 2011]. In SqueeSAR algorithm, combination of PS and DS helps to work in rural areas, where the coherency is lower. In Navarro-Sanchez and Lopez-Sanchez [2013] a similar algorithm, with contribution of polarimetric based radar data, was heuristically proposed.

All the different PSI implementations described above, however, share some main features, that are described in the following. In all of them, a large stack of radar images are considered for estimation of historical changes of the Earth surface's, with proper modeling techniques. The output of PSI algorithms are deformation time series of the scatterers, and the elevation of those scatterers. PSI technique exploits the fact that some radar's pixels remain coherent during the time. With this method and by using a large stack of SAR images (usually more than 20 SAR images), atmospheric errors (i.e., the Atmospheric Phase Screen, APS) can be estimated with sufficient accuracy, and the proper phase correction can be implemented to remove them. In the standard PSI methodologies, a single master image with specific criteria is selected (from N given images), and (N - 1) differential interferograms w.r.t. the master image are generated. Then, with different approaches, Permanent Scatterers Candidates

(PSCs) are selected. By refinements of the selected PSCs, and by using Permanent Scatterers Potentials (PSPs) [Kampes, 2005], final Permanent Scatterers (PSs) can be generated. For each PS point, time series of the historical records of the Earth surface's height changes, and the height of each PS with respect to a reference point, are measurable. This methodology shows promising results in urban areas, where it is able to achieve an average of 100 PSs/(points densities) with low resolution sensors like ERS1/2 and ENVISAT-ASAR, and an average of a couple of thousands PSs/with high resolution sensors like TerraSAR-X and Cosmo-SkyMed. On the contrary, the rural/vegetated areas might not be explored properly with PSI methodology. The main reason is the absence of proper stable scatterers in such areas. Another disadvantage of the PSI is the need for a minimum amount of images for making appropriate phase unwrapping steps, which could severely influence the degree of correctness of the selected PSC. The other limitation of InSAR time series methodologies, is that PSI (and SBAS too) is a relative technique, i.e., all of the calculated time series for PS points are measured w.r.t. a reference point, which is assumed to be without any kind of movements. Nonetheless, many promising methodologies, like continuous GPS or leveling, could resolve this problem properly [Ketelaar, 2009]. Another limitation is mainly due to the observation geometry of the satellite systems. PSI deformation rates are only measured along the satellite Line Of Sight (LOS) direction; therefore, the obtained value of the deformation is actually just the projection of the deformation vector onto the SAR look direction.

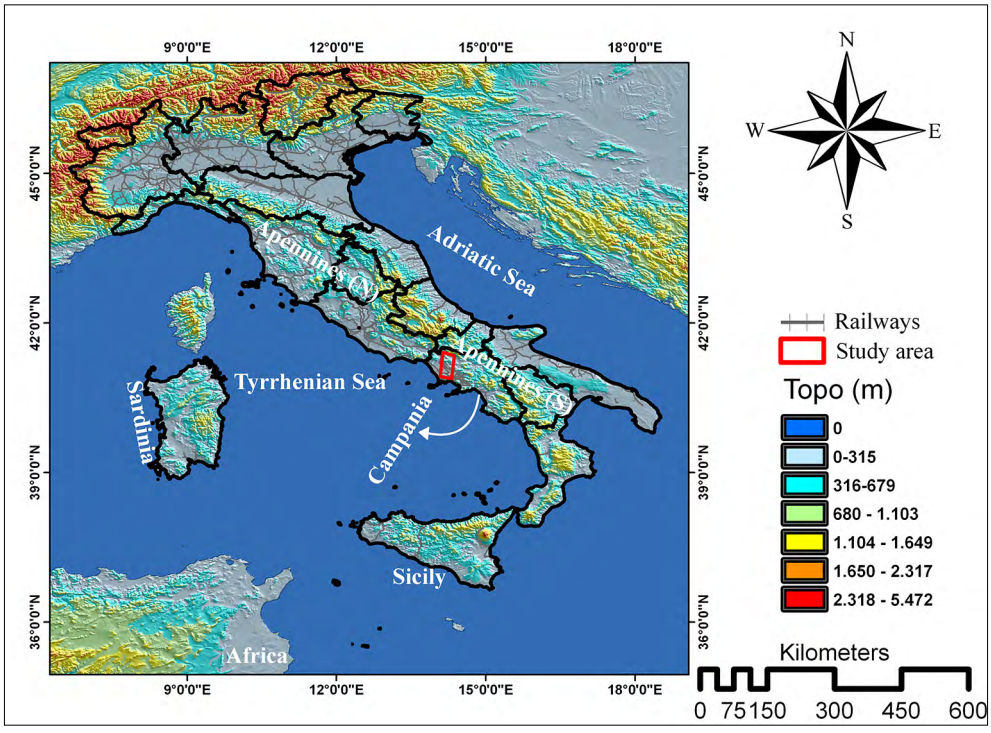

Figure 1 - Campania region (Italy) and the study area.

In this paper we apply the DInSAR PS technique to the remote monitoring of railways in the Campania region (Italy). In particular, we are interested in monitoring a bridge over the Volturno river, at Triflisco. As widely reported in literature [Calcaterra et al., 2003; Vilardo et al., 2009; Del Prete et al., 2010; Blonda et al., 2012; Parise and Vennari, 2013], Campania region is very unstable in terms of the Earth surfaces' deformations. Therefore this area must go under geo-based investigation periodically. In addition, in the Campania region, the railways and bridges are pretty old, and are prone to sudden or slow deformation threats. For instance, the bridge over the Volturno river and the railways considered in this study were made in 1953. To evaluate possible deformation of this bridge, employment of high resolution Cosmo-SkyMed radar images is proposed, and an InSAR/PSI analysis has been carried out. The results presented here show fairly stable conditions on the studied railways and the main targeted bridge, with thermal periodical deformation.
In the following sections, first we describe the study area, then we proceed to briefly illustrate the applied methodology, and finally we present and discuss obtained results.

Study area

The Campania region includes the Campania plain as a Northwest-Southeast elongated structure (see Fig. 1) delimited at north, south and east by the Apennines chain (see Fig. 1). To the west, the Campania region is bounded by the Tyrrhenian Sea. Intense urbanization, active volcanoes, complicated fault systems, landslides, subsidence, and hydrological instability (flooding) are the characteristics of this region [Calcaterra et al., 2003; Vilardo et al., 2009; Del Prete et al., 2010; Blonda et al., 2012; Parise and Vennari, 2013]. 246 out of 652 sinkholes (38%) of entire Italy are located in Campania region itself [Parise and Vennari, 2013]. Volcanism is very developed in this area and is observed at Roccamonfina, Ischia, Vesuvius, and Phlegraean Fields regions. Historical eruptions happened at Vesuvius (several, the last one in 1944 A.D.), Ischia (1302 A.D.), and Phlegraean Fields (1538 A.D.).
Complicated fault systems are developed in Campania, which can be observed in many locations. Complicated behavior of the hydrothermal systems played a key role in triggering of seismicity, uplift and subsidence in Vesuvius, Ischia, and Phlegraean Fields. Many destructive historical earthquakes happened in Campania: 1930 (Ms=6.7), 1962 (Ms=6.2), 1980 (Ms=6.9). Most of the previous studies from Leveling, GPS, and SAR data are concentrated on the volcanic areas like Vesuvius, and Napoli city itself. Conversely, we are here interested in the area at north of Napoli, including the Volturno river and a local railway, see Figure 2, with a bridge at Triflisco on which our interest is mainly focused. This bridge over the Volturno river and the entire railway considered in this study were made in 1953. In order to increase the stability of this bridge, the local railway company (EAV) made some rock bolts installations and cement injections to make the three pillars of the bridge more stable. Despite these efforts, EAV still was interested to evaluate the probable geophysical change of the railways (deformation rates) with other independent methods like InSAR and PSI.

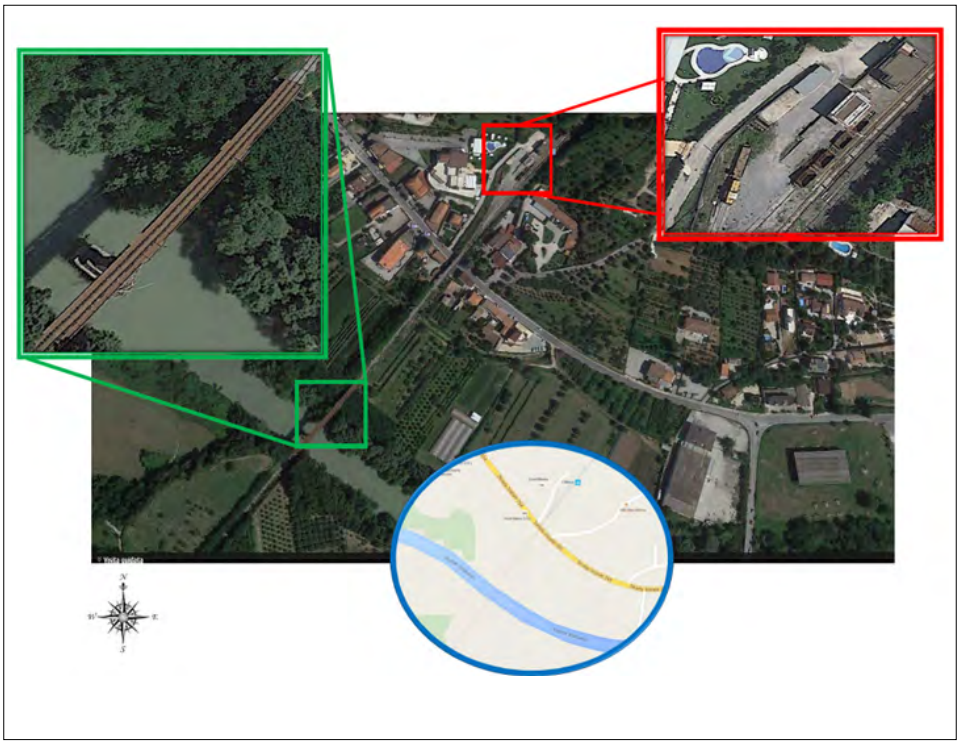

Figure 2 - Study area, railways, targeted bridge, and Volturno river are depicted in this figure. Down in the middle a global view of the study area is depicted (from google map). On top left, the targeted bridge of the Volturno river, and on the top right, the train station are enlarged.

Methodology

Several different algorithms for PSI methodologies have been proposed in the last 15 years, but most of them follow this standard routine/mechanism [Kampes, 2005]:

I. Generation of the interferograms based on the available InSAR imageries;
II. Generation of differential interferograms using a Digital Elevation Model (DEM) and orbit data;
III. Selection of Permanent Scatterer Candidates (PSC);
IV. Refinement of PSCs to get the real PSs with different methodologies and phase unwrapping;
V. Repeating of the steps from I to IV, with Permanent Scatterer Potentials (PSPs) to densify (compact) the PSs network.

Producing of InSAR interferograms from InSAR imageries is the fundamental concept of PSI analysis. For N available InSAR images, $N - 1$ interferogrms could be generated with respect to the selected master (m) image. There are number of different methodologies to select the master image from the entire set of radar images. The most important one is based on minimization of the dispersion of the perpendicular baseline. In Kampes [2005] also another methodology based on maximization of coherence of interferometric stack is presented. In this work, we perform a heuristic minimization of the perpendicular and

temporal baseline dispersion: we visually select the most central image in the graph of temporal/perpendicular baselines, shown in Figure 3.
After selection of the master image (m) and generation of interferograms, a DEM and precise orbit data must be used to generate $N-1$ differential interferograms from N radar images. The differential phase equation for a differential interferogram reads:

$$\Phi = \varphi_{atm} + \varphi_{orb} + \varphi_{def} + \varphi_{scat} + \varphi_{DEM} + \varphi_n \quad [1]$$

We are interested in the surface displacement component of the total observed phase (φ_{def}). Other contributions to the total observed phase are the topographic contribution φ_{DEM}, and the orbital error φ_{orb}, that can be minimized using precise orbit data. The atmospheric contribution, φ_{atm} is related to the APS, and φ_{scat} is the change in the scattering attributes over the time. Usually, the scattering component is small in manmade objects (like railways). Finally φ_n is the noise component of the phase, which for strong scatterers should be negligible. With selection of proper DEM data, and precise orbit data, the topographic and orbital phase components in general phase equation would be handled properly.
Amplitude dispersion index D_a is used to generate the first rank Persistent Scatterer Candidate (PSC). This index is defined as the ratio of standard deviation σ_a and temporal mean $< a >$ of the pixel's (temporal) amplitudes a, and it can be also approximately related to the phase standard deviation σ_φ [Ferretti et al., 2001]:

$$D_a = \frac{\sigma_a}{< a >} \cong tan\left(\sigma_\varphi\right) \cong \sigma_\varphi \quad [2]$$

where the last approximate equality holds for small values of σ_φ (i.e. $\sigma_\varphi < 0.25$).
Points for which this index is smaller than a prescribed user-defined threshold are selected. The choice of the threshold for D_a may depend on the number of images, but usually it lies in the range from 0.2 to 0.3. [Ferretti et al., 2001] The selected points (PSCs) are used to make the first rank network. Assume that φ_i^{ms} is the interferometric phase difference between master (m) and slave (s) imageries, for persistent scatterer in position i. At the beginning, the phase difference φ_i^{ms} is ambiguous -wrapped- and should be unwrapped to get the actual -physically meaningful- amount of phase.
The first "interpretable" PSI observation is the double-difference φ_{ij}^{ms}, which is the difference between φ_i^{ms} and φ_j^{ms}, where i and j are two different PSs, so that it is represented both in temporal and spatial domains simultaneously. This implies that PSI observations require a determined spatial and a temporal reference basis, i.e., a reference point (selected in an area that can be considered fixed) and a reference time (i.e., the master acquisition, as already described) must be selected, and all deformations must be intended with respect to that point and that time. The number of independent double-differences that can be formed from the original phase observations is equal to $(N-1) \times (P-1)$, for N InSAR acquisitions and

P PSs. By maximization of the ensemble coherence w.r.t. the double difference phase and the phases related to the modeled height and velocity, we are able to measure the height and speed of deformation on each network's branches. After finding these parameters (i.e., height of scatterers and speed of deformation), the only remaining task is the proper phase unwrapping of the phase, that can be carried out by using one of the many well-known unwrapping methodologies (see e.g., Usai et al. [1999] and Kampes [2005]). Densification of PSs is then performed by iterating previous steps.

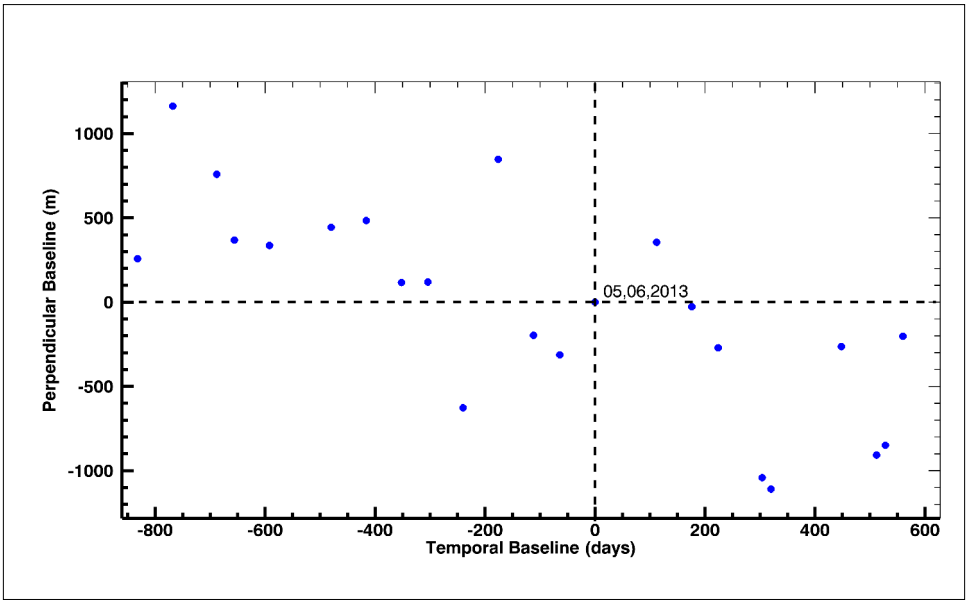

Figure 3 - Perpendicular and temporal baselines. The image acquired on 2013 06 05 has been selected as the master image.

Results and discussions

The study area has already gone under PSI analysis with low resolution images like ERS, and ENVISAT-ASAR from PlaneTek Company before [Nutricato and Nitti, 2015]. However, with these sensors, the number of PSs in the study area is too small. For instance, on the bridge over the Volturno river considered in this study, with ERS data sets from 1992 till 2000, in the ascending mode, only two, and, with the descending mode, only one PS have been selected. With ENVISAT-ASAR sensor in temporal baseline of 2003-2010, in the ascending mode six, and in the descending mode only one PS have been selected. Therefore, the need for using high resolution imageries for a better understanding of the deformation phenomena on the bridge is obvious.

Table 1 - Available CSK data sets (from same sensor of CSK4_HI01), and perpendicular, temporal, and Doppler baselines. Image number 14 (20130605) has been selected as the master image.

Nr	Acquisition Date	Perpendicular Baselines [m]	Temporal Baselines [day]	Doppler Baselines [Hz]
1	20110224	252.5	-832	-46.33
2	20110429	1153.2	-768	-10.17
3	20110718	750.6	-688	-36.37
4	20110819	363.4	-656	-99.25
5	20111022	332.5	-592	-129.48
6	20111225	1472.9	-528	-72.75
7	20120211	438	-480	-65.46
8	20120415	479.8	-416	-11.3
9	20120618	113.1	-352	41.41
10	20120805	115.9	-304	-64.35
11	20121008	-623.4	-240	4.25
12	20121211	840	-176	-13.34
13	20130213	-196	-112	-7.23
14	20130402	-314.1	-64	-35.47
15	20130605	0	0	0
16	20130925	353.8	112	-2.92
17	20131128	-28.5	176	30.86
18	20140115	-266.4	224	15.19
19	20140405	-1034	304	43.15
20	20140421	-1102.5	320	-29.88
21	20140827	-263.7	448	3.75
22	20141030	-900	512	-8.94
23	20141115	-841.4	528	32.66
24	20141217	-201.3	560	6.62
25	20150323	348.6	656	69.11

Accordingly, 25 InSAR images of Cosmo-SkyMed sensors at descending mode of HIMAGE/Stripmap were used for our study area, (it is depicted in Fig. 1 as a red rectangle). Images are acquired in HH polarization, right looking, X-band (EM wavelength: 3.1228 cm), with mean incident angle of 26.60 degrees (incidence angle at the center of the transmitted beam). Data cover a temporal baseline between February 24 2011 till March 23

2015. We examine this stack of images to identify the number of scatterers on the ground that consistently/permanently show stable reflections back to the satellite on all images in the temporal baseline. With PSI analysis historical motion of the permanent scatterers on the ground was determined. Image of 5th June of 2013 (see Tab.1) has been selected as master image (see Fig. 3), and radar images were cropped in an area as big as $7.5 \times 7.5\ km^2$, centered at the bridge on Volturno river (Fig. 2). Then, 24 differential interferograms have been generated w.r.t. the master image. With Cosmo-SkyMed data sets and for the selected study area of $7.5 \times 7.5\ km^2$, more than 190,000 PSs including some on the railways, and some on the bridge of Volturno River have been selected. The average velocity and ensemble coherence are as big as -1.8 mm/yr (for whole area) and 73%, respectively, and the density of selected PSs is equal to 3378 PSs/ km^2 for entire area.

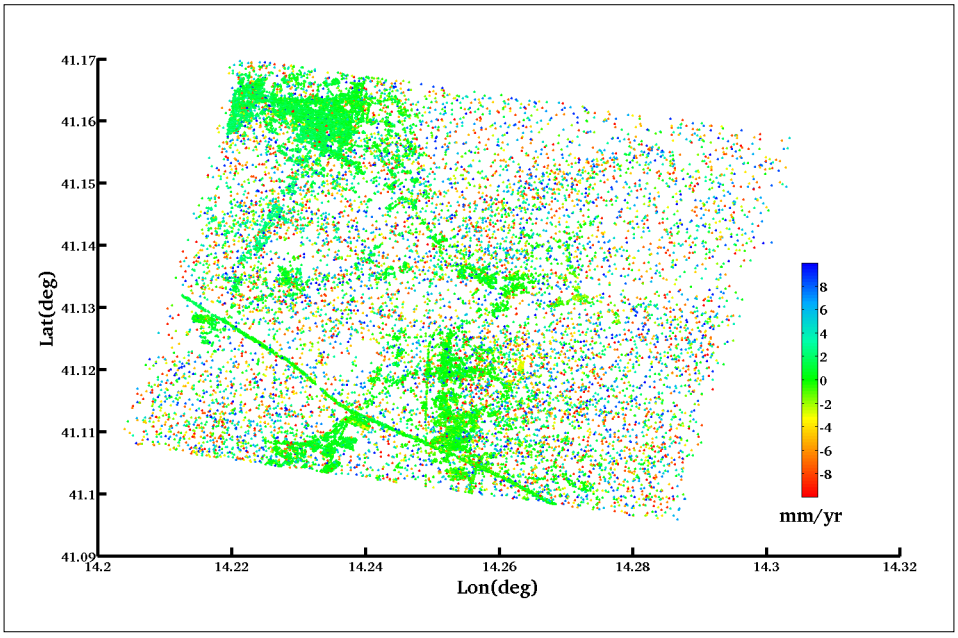

Figure 4 - Mean surface displacement velocity of the study area based on 25 InSAR images from 2011 02 24 until 2015 03 23, estimated with PSI methodology. Colored pixels are PSs, white pixels are not PSs and no velocity estimation is obtained for them.

The majority of the PSs are from man-made structures like houses, highways, railways, etc. Figure 4 shows the mean velocity (deformation rate) of the Earth surface's in the study area. As it is clear from this figure, man-made structures like highways, railways, and cities are designated as potential permanent radar wave reflectors (i.e. PSs).

Figure 5 shows the selected scatterers (PSs) on the railways and the bridge itself. It turns out that they are 1385 and, as it is obvious from this figure, most of them are stable. Minimum and maximum displacement rates are -9.58 mm/yr and 9.97 mm/yr, respectively, but these high values are only obtained in some isolated points (blue or red dots in Fig. 5), surrounded by points for which the displacements rates are much lower (green dots), so that they are

probably due to phase noise. The velocity averaged over all the 1385 PSs is 1.8 mm/yr, and standard deviation (SD) is 3.57 mm/yr. The PSs on the railways and nearby structures are selected in the GIS environment manually. Thirty of these PSs are located on the bridge, and they are highlighted by an ellipse in Figure 5. For these 30 PSs, minimum and maximum velocities of – 0.9 and 0.05 mm/yr have been observed, respectively, with average of – 0.3 mm/yr and SD=0.3 mm/yr.

For each PS, not only the displacement rate, but also the entire time series of displacements is obtained. For instance, in Figure 6, the time series of six PSs, out of the 30 PSs on the bridge, have been depicted. This allows us a deeper analysis of the bridge displacements' behaviour. In particular, we have compared the time variations of the bridge displacement (or deformation) with the time variations of temperature in the same considered area and in the same time interval.

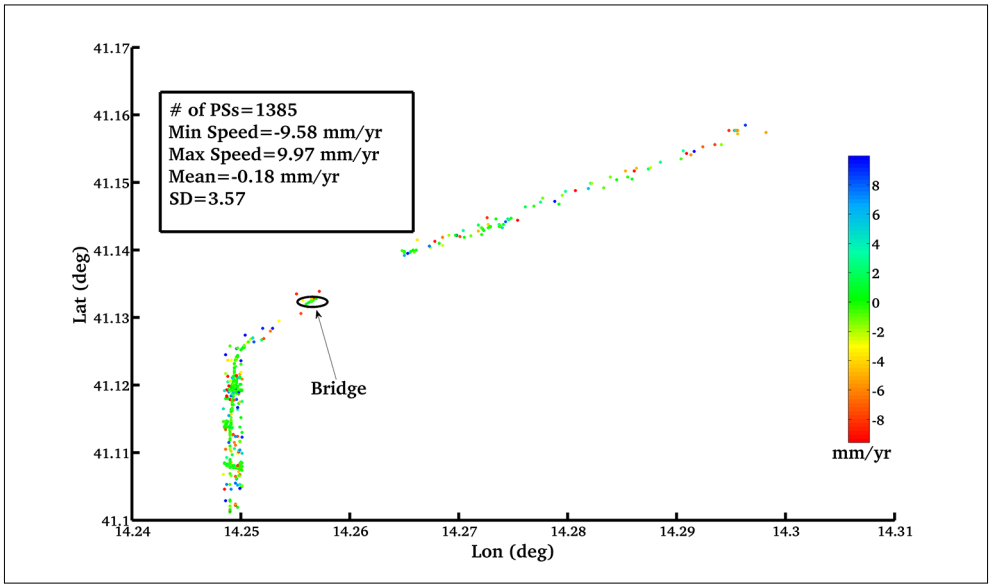

Figure 5 - Mean displacement rates of PSs on the railways and statistics of these PSs.

In Figure 7, the green line shows the deformation time series averaged over the 30 PSs' on the bridge, and the blue points represent the temperature in the Neapolitan metropolitan area (http://www7.ncdc.noaa.gov/CDO/cdoselect.cmd?datasetabbv=GSOD&countryabbv=&georegionabbv=). As it is obvious from this figure, the deformation and temperature time series are very similar, demonstrating that most of the deformation is cyclical and it is related to the temperature seasonal changes in winter and summer time. Decreasing of the detected amplitude of deformation yearly cycle in 2013 and 2014 (Fig. 7) is actually probably due to undersampling: in fact, it is related to the smaller number of the images in that period, with no image acquired in summer 2013 and only one (at the end of August) in summer 2014.

In conclusion, comparison of average PSs time series on the bridge with thermal data shows

that most of the Line Of Sight (LOS) changes are due to the periodical variations of the temperature (i.e., winter and summer), with cyclical, seasonal deformations superimposed to a small rate of deformation of -0.30 mm/yr.

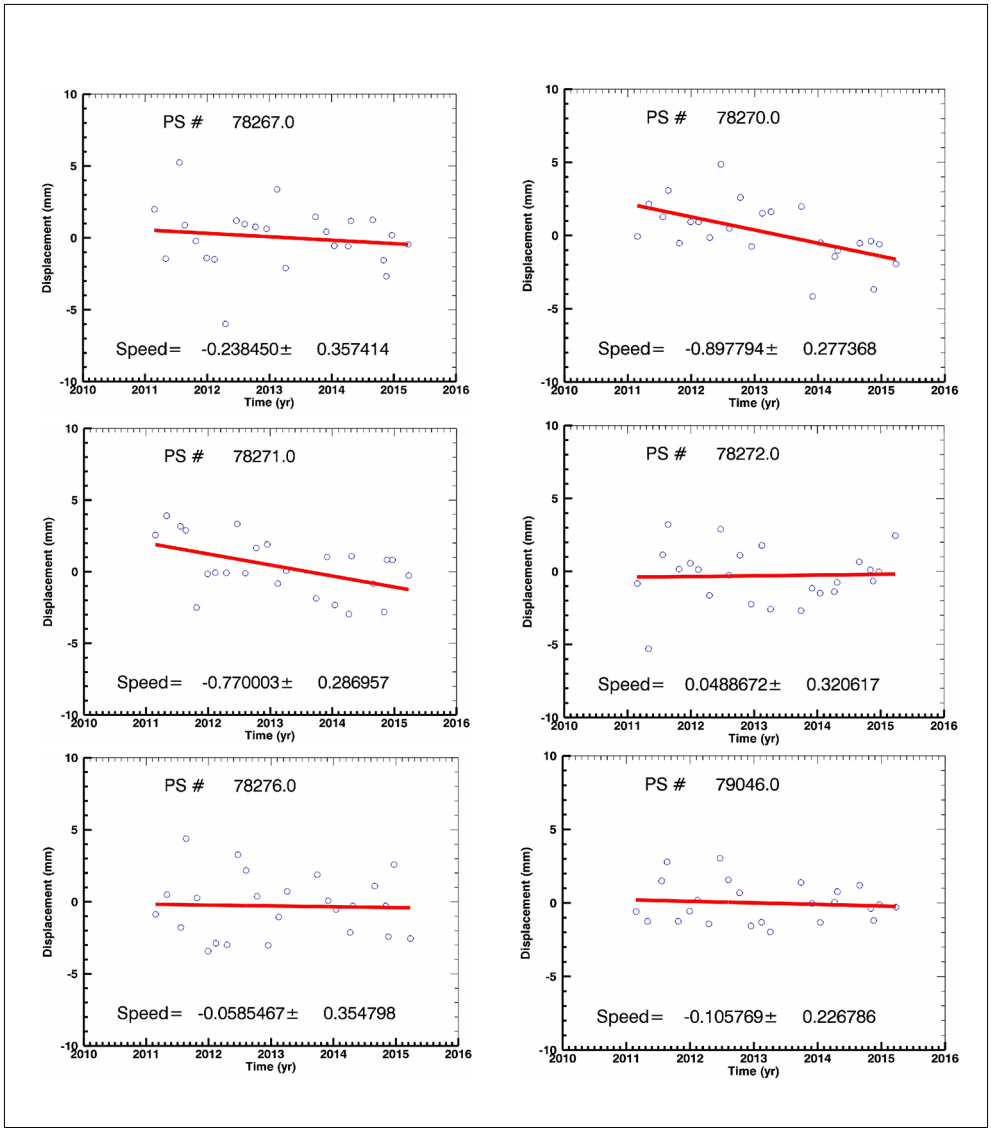

Figure 6 - Six time series of the surface deformations on the Volturno river's bridge (speed is expressed in mm/year).

Accordingly, use of higher resolution imageries like CSK and TSX to have better and smooth time series has been demonstrated by using CSK data. However, combination of descending mode with ascending mode imageries to achieve the deformation rates in both

vertical and horizontal directions (i.e., not only along the line of sight), continuous GPS deformation monitoring, corner reflector establishment, and leveling data might improve understanding of this study area. Comparison of SBAS methodology with the employed PSI technique also would be helpful and is the subject of current study.

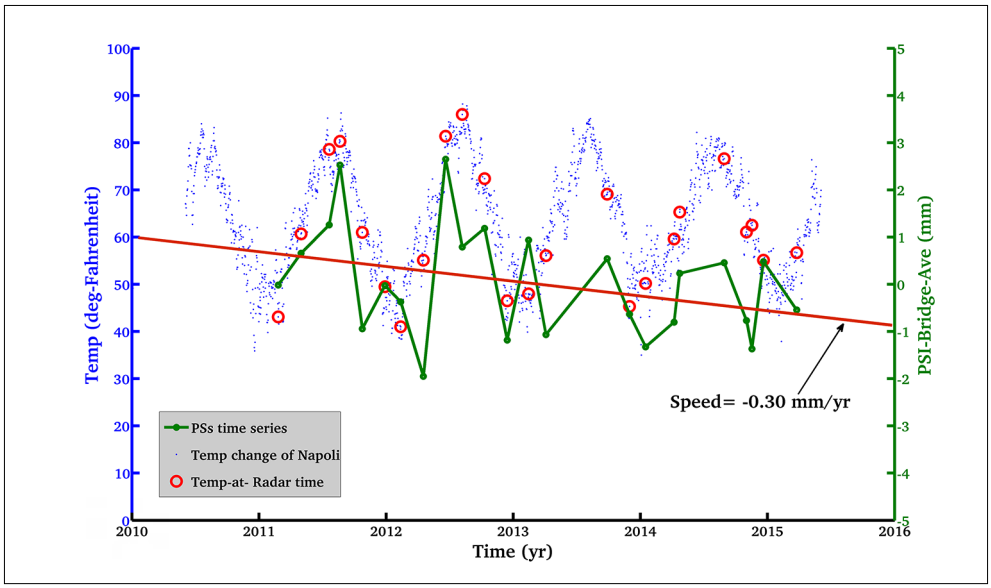

Figure 7 - Bridge deformation as a function of time (green points) compared with temperature of the Neapolitan metropolitan area as a function of time (blue points). Bridge deformation is obtained by averaging the values of all the 30 PSs on the bridge, and temperature data are taken from NOAA.

Conclusion

Monitoring stability of the railways in Campania (Italy) by using the DInSAR technique is the subject of this work. We analyzed 25 X-band radar images of Cosmo-SkyMed satellite from Campania during the time span of February 24 2011 till March 23 2015, with InSAR and PSI methodologies. We have focused our analysis on a railway, and in particular on a railway bridge over the Volturno river, at Triflisco. The use of higher resolution imagery has allowed us obtaining a much larger number of persistent scatterers with respect to previous studies on the same area, so that more reliable results have been obtained. In the average of more than 190 thousands of persistent scatterers, velocities and ensemble coherence are as big as –1.8 mm/yr and 73% respectively.

On the bridge over the Volturno river (the main target), 30 PSs have been obtained. In the studied time series, minimum velocity of –0.9 and maximum of 0.05 mm/yr with average of –0.3 mm/yr and SD=0.3 mm/yr have been observed, demonstrating very stable and safe conditions on the bridge.

Comparison of average PSs time series on the bridge with thermal data shows that most of the Line Of Sight (LOS) changes are due to the periodical, seasonal variations of the temperature (i.e., winter and summer).

In conclusion, our five year spanning SAR data analysis shows the importance and capability of InSAR/PSI methodologies for deformation rate evaluation. However, an important finding of our study is that the availability of high-resolution X-band SAR data is a key need for interferometric approaches if we want to monitor deformation rates of infrastructures. In addition, it should be pointed out that, due to limited (re)visiting and SAR viewing geometries, PSI is not always capable of providing a real-time warning of possible critical deformations that might be occurred on the railways, so that for this latter aim PSI should be employed in conjunction with other monitoring methods.

Acknowledgments

This work has been supported by the project "MODISTA - Soluzioni innovative per il Monitoraggio e la Diagnostica preventiva di infrastrutture e flotte di veicoli da remoto al fine di elevare i livelli di disponibilità, efficienza e sicurezza dei siSTemi ferroviAri", Project code: PON03PE_00159_6.

References

Berardino P., Fornaro G., Lanari R., Sansosti E. (2002) - *A new algorithm for surface deformation monitoring based on small baseline differential SAR interferograms*. IEEE Transactions on Geoscience and Remote Sensing, 40: 2375-2383. doi: http://dx.doi.org/10.1109/TGRS.2002.803792.

Blonda P., Parise M., Reichenbach P., Guzzetti F. (2012) - *Rock-fall hazard assessment along a road in the Sorrento Peninsula, Campania, southern Italy*. Natural Hazards, 61 (1): 187-201. doi: http://dx.doi.org/10.1007/s11069-011-9899-0.

Calcaterra M., Parise M., Blonda P. (2003) - *Combining historical and geological data for the assessment of the landslide hazard: a case study from Campania, Italy*. Natural Hazards and Earth Systems Sciences, 3 (1/2): 3-16. doi: http://dx.doi.org/10.5194/nhess-3-3-2003.

Crosetto M., Crippa B., Biescas E. (2005) - *Early detection and in-depth analysis of deformation phenomena by radar interferometry*. Engineering Geology, 79: 81-91. doi: http://dx.doi.org/10.1016/j.enggeo.2004.10.016.

Crosetto M., Biescas E., Duro J., Closa J., Arnaud A. (2008) - *Generation of advanced ERS and ENVISAT interferometric SAR products using the stable point network technique*. Photogrammetric Engineering and Remote Sensing, 74: 443-450. doi: http://dx.doi.org/10.14358/PERS.74.4.443.

Del Prete S., Di Crescenzo S., Santangelo N., Santo A. (2010) - *Collapse sinkholes in Campania (southern Italy): predisposing factors, genetic hypothesis and susceptibility*. Geomorphology, 54: 259-284. doi: http://dx.doi.org/10.1127/0372-8854/2010/0054S2-0014.

Ferretti A., Prati C., Rocca F. (2001) - *Permanent scatterers in SAR interferometry*. IEEE Transactions on Geoscience and Remote Sensing, 39 (1): 8-20. doi: http://dx.doi.org/10.1109/36.898661.

Ferretti A., Fumagalli A., Novali F., Prati C., Rocca F., Rucci A. (2011) - *A new algorithm for processing interferometric data-stacks: SqueeSAR*. IEEE Transactions on Geoscience and Remote Sensing, 49: 3460-3470. doi: http://dx.doi.org/10.1109/TGRS.2011.2124465.

Ferretti A., Prati C., Rocca F. (1999a) - *Multibaseline InSAR DEM Reconstruction: The Wavelet Approach*. IEEE Transactions on Geoscience and Remote Sensing, 37 (2): 705-715. doi: http://dx.doi.org/10.1109/36.752187.

Ferretti A., Prati C., Rocca F. (1999b) - *Non-Uniform Motion Monitoring Using the Permanent Scatterers Technique*. In: Second International Workshop on ERS SAR Interferometry, 'FRINGE99', Liege, Belgium, 10-12 Nov 1999, pp. 1-6, ESA.

Ferretti A., Prati C., Rocca F. (2000) - *Nonlinear subsidence rate estimation using permanent scatterers in differential SAR interferometry*. IEEE Transactions on Geoscience and Remote Sensing, 38: 2202-2212. doi: http://dx.doi.org/10.1109/36.868878.

Ferretti A., Prati C., Rocca F. (2001) - *Permanent scatterers in SAR interferometry*. IEEE Transactions on Geoscience and Remote Sensing, 39, 8-20. doi: http://dx.doi.org/10.1109/36.898661.

Hooper A., Zebker H., Segall P., Kampes B. (2004) - *A new method for measuring deformation on volcanoes and other natural terrains using InSAR persistent scatterers*. Geophysical Research Letters, 31 (23). doi: http://dx.doi.org/10.1029/2004GL021737.

Hooper A. (2008) - *A multi-temporal InSAR method incorporating both persistent scatterer and small baseline approaches*. Geophysical Research Letters, 35 (L16302). doi: http://dx.doi.org/10.1029/2008gl034654.

Kampes B. (2005) - *Displacement parameter estimation using permanent scatterer interferometry*. Ph.D. thesis, Technische Universiteit Delft.

Ketelaar V.B.H. Gini (2009) - *Satellite Radar Interferometry* Remote Sensing and Digital Image Processing, 14, Springer Business Media B.V.

Lanari R., Mora O., Manunta M., Mallorqui J.J., Berardino P., Sansosti E. (2004) - *A small-baseline approach for investigating deformations on full-resolution differential SAR interferograms*. IEEE Transactions on Geoscience and Remote Sensing, 42: 1377-1386. doi: http://dx.doi.org/10.1109/TGRS.2004.828196.

Mora O., Mallorqui J.J., Broquetas A. (2003) - *Linear and nonlinear terrain deformation maps from a reduced set of interferometric SAR images*. IEEE Transactions on Geoscience and Remote Sensing, 41: 2243-2253. doi: http://dx.doi.org/10.1109/TGRS.2003.814657.

Navarro-Sanchez V.D., Lopez-Sanchez J.M. (2013) - *Spatial adaptive speckle filtering driven by temporal polarimetric statistics and its application to PSI*. IEEE Transactions on Geoscience and Remote Sensing, 99: 1-10.

Nutricato R., Nitti D.O. (2015) - *Processamento di scene Cosmo-SkyMed con tecniche di interferometria differenziale PS*. Internal report in Italian.

Parise M., Vennari C.A. (2013) - *Chronological catalogue of sinkhole in ITALY: The first step toward a real evaluation of the sinkhole hazard.* 13th sinkhole conference NCKRI SYMPOSIUM 2013.

Pepe A., Manunta M., Mazzarella G., Lanari R. (2007) - *A space-time minimum cost flow phase unwrapping algorithm for the generation of persistent scatterers deformation time-series*. Proceedings of the IEEE International Geoscience and Remote Sensing Symposium, Barcelona, Spain, 23-28 July 2007. doi: http://dx.doi.org/10.1109/igarss.2007.4424055.

Pepe A., Sansosti E., Berardino P., Lanari R. (2005) - *On the generation of ERS/ENVISAT D-InSAR time-series via the SBAS technique*. IEEE Geoscience and Remote Sensing

Letters, 2: 265-269. doi: http://dx.doi.org/10.1109/LGRS.2005.848497.

Pepe A., Berardino P., Bonano M., Euillades L.D., Lanari R., Sansosti E. (2011) - *SBAS-based satellite orbit correction for the generation of DInSAR time-series: Application to RADARSAT-1 data*. IEEE Transactions on Geoscience and Remote Sensing, 49: 5150-5165. doi: http://dx.doi.org/10.1109/TGRS.2011.2155069.

Perissin D., Ferretti A., Piantanida R., Piccagli D., Prati C., Rocca F., Rucci A., de Zan F. (2008) - *Repeat-pass SAR interferometry with partially coherent targets*. Fifth International Workshop on ERS/Envisat SAR Interferometry, 'FRINGE07', Frascati, Italy, 26 Nov-30 Nov 2007, pp. 6.

Usai S., Hanssen R. (1997) - *Long time scale INSAR by means of high coherence features*. Third ERS Symposium-Space at the Service of our Environment, Florence, Italy, 17-21 March 1997, pp. 225-228.

Usai S., Klees R. (1999a) - *On the interferometric characteristics of anthropogenic features*. International Geoscience and Remote Sensing Symposium, Hamburg, Germany, 28 June-2 July 1999. doi: http://dx.doi.org/10.1109/igarss.1999.772078.

Usai S., Klees R. (1999b) - *SAR Interferometry on Very Long Time Scale: A Study of the Interferometric Characteristics Of Man-Made Features*. IEEE Transactions on Geoscience and Remote Sensing, 37 (4): 2118-2123. doi: http://dx.doi.org/10.1109/36.774730.

Vilardo G., Ventura G., Terranova C., Matano F., Nardo S. (2009) - *Ground deformation due to tectonic, hydrothermal, gravity, hydrogeological, and anthropic processes in the Campania Region (Southern Italy) from Permanent Scatterers Synthetic Aperture Radar Interferometry*. Remote Sensing and Environments, 113 (1): 197-212. doi: http://dx.doi.org/10.1016/j.rse.2008.09.007.

Werner C., Wegmüller U., Strozzi T., Wiesmann A. (2003) - *Interferometric point target analysis for deformation mapping.* Proceedings of the 2003 Geoscience and Remote Sensing Symposium, Toulouse, France, 21-25 July 2003. doi: http://dx.doi.org/10.1109/igarss.2003.1295516.